International Journal on Advanced Science Engineering Information Technology

Vol.12 (2022) No. 6
ISSN: 2088-5334

Flood Vulnerability Evaluation and Prediction Using Multi-temporal Data: A Case in Tangerang, Indonesia

Budi Heru Santosa [a, b], Dwi Nowo Martono [a,*], Rachmadhi Purwana [a], Raldi Hendro Koestoer [a, c]

[a] *School of Environmental Science, University of Indonesia, Kampus UI Salemba, Jl. Salemba Raya No. 4, Jakarta Pusat, 10430, Indonesia*
[b] *The National Research and Innovation Agency (BRIN), Gedung B.J. Habibie, Jl. M.H. Thamrin No. 8, Jakarta Pusat, 10340, Indonesia*
[c] *Coordinating Ministry for Economic Affairs of the Republic of Indonesia, Jl. Lap. Banteng Timur No. 2-4, Jakarta Pusat, 10710, Indonesia*
*Corresponding author: *dwi.nowo11@ui.ac.id*

***Abstract*— Land-use change has an impact on growing physical flood vulnerability. Geographic Information System (GIS) and Analytic Hierarchy Process (AHP) approaches are increasingly being used for flood vulnerability assessments. However, none has used time-series land cover data for evaluation and rainfall over various return periods for prediction simultaneously, especially in Indonesia. Therefore, this study aims to evaluate and predict physical flood vulnerability using time-series land cover data and rainfall data over various return periods. Eight criteria were considered in the assessment: elevation, topographic wetness index, slope, distance to the river, distance downstream, soil type, rainfall, and land cover. The criteria weights were determined using the AHP method based on expert judgment. The multi-criteria model was built and validated using flood inundation data. Based on the validated model, the effect of land cover changes on flood vulnerability was evaluated. The flood vulnerability changes were also predicted based on rainfall over various return periods. The evaluation and prediction models have shown reliable findings. The criterion elevation and distance to the river significantly influenced the physical flood vulnerability by 41% and 20%. The evaluation model showed a strong correlation between the built-up area and the area with high flood vulnerability ($r^2 = 0.96$). Furthermore, the model predicted an inundation area expansion for rainfall over various return periods. Further research using spatial data with higher resolution and more advanced validation techniques is needed to improve the model accuracy.**

***Keywords*—Flood vulnerability; multi-criteria; GIS; weighted overlay; flood inundation.**

Manuscript received 21 Dec. 2021; revised 19 May 2022; accepted 23 Jul. 2022. Date of publication 31 Dec. 2022.

I. INTRODUCTION

Due to urbanization, land use transition negatively affects local ecological systems [1], [2]. As a result, the ecological function of green space to achieve a livable city decreases linearly with the green space reduction [3]. If this phenomenon occurs rapidly, the pressure on green space and water resources will cause negative impacts on the environment [4]. The changes in green space and land to accommodate flood discharge into the built-up area increases the maximum discharge and the damage in a flood-affected area [5]. Land-use change and climate change impacts also increase watershed vulnerability to flooding, so local authorities need to evaluate the flood vulnerability [6]. This condition is experienced by Tangerang City in Indonesia, a fast-growing city with a tropical climate adjacent to Jakarta, the capital city of Indonesia.

Tangerang City has experienced land-use changes due to the regional physical development policy [7]. The built-up area has increased rapidly in the last decades, whereas the vegetated land area has decreased. As a result, floods occur with greater frequency and greater strength. The local authorities have prepared a Drainage System Master Plan to overcome the flood problem, including developing flood control infrastructure [8]; nevertheless, in 2020, the city has suffered significant losses due to flooding. Based on this condition, the local authorities need to evaluate the flood vulnerability due to land-use changes as an impact of the physical development in the area. They also need flood vulnerability prediction models in several rainfall scenarios with a return period of up to 100 years. However, the local authorities often face a dearth of data on flood discharge, as required by hydrological and hydraulic models for validation purposes [9]. This condition causes difficulty in implementing hydrological and hydraulic models because the model's accuracy cannot be proven. Instead, scholars implement the

watershed physical vulnerability theory by accommodating the physical factors that influence physical flood vulnerability [10].

A large body of literature has discussed the GIS and multi-criteria decision-making (MCDM) approach for mapping and measuring physical flood vulnerability. Over the last three decades, remote sensing and GIS approaches have been successfully applied to various flood vulnerability assessments [11], [12], [21], [13]–[20]. The free availability of medium-resolution remote sensing data also supported the increased use of geospatial in flood vulnerability analysis. Some authors used the free available remote sensing data, such as Landsat [15], [17], [20] and Sentinel [13] imagery data, Digital Elevation Model (DEM) Shuttle Radar Terrain Mission (SRTM) [13], [19], and The Terra Advanced Spaceborne Thermal Emission and Reflection Radiometer (ASTER) imagery data [17], [18], as primary data for constructing several physical vulnerability factors.

Studies have applied a combination of geospatial and MCDM approaches [11]–[13], [16], [20]; other studies combined the GIS approach with the random forest method [22], [23], and the fuzzy approach [24]–[26]. However, to the best of the author's knowledge, none has used historical land cover data for evaluation and rainfall data over various return periods to predict flood vulnerability simultaneously. In most studies, the different roles of each physical criterion on flood vulnerability were considered by applying criteria weights in the analysis process. In most studies, a single data package was analyzed so that the resulting flood vulnerability map was suitable for one particular condition [11]–[13]. Feloni et al. [12] used one dataset with variations in the weighting of the criteria in the multi-criteria decision-making method to find the best method of weighting the criteria. Deepak et al. [10] and Hussain et al. [13] also used one dataset to find the effect of flood vulnerability criteria on physical flood vulnerability. Using one dataset, the assessment results should only represent one physical condition in the study area. Therefore these results could not meet the need of local authorities to support flood adaptive spatial planning [27] and educate the community regarding the potential flood [28], [29]. This study fills this research gap by evaluating flood vulnerability based on time-series land cover data and predicting flood vulnerability using rainfall over various return periods.

Using the Kali Ledug Watershed in Tangerang city, Indonesia, as a study area, this research aims to evaluate and predict physical flood vulnerability using time-series land cover data and rainfall data over various return periods. The evaluation and prediction results would support the local authorities and other stakeholders as a reference in flood adaptive city spatial planning and as a communication tool for public education regarding flood risk management.

II. Materials and Method

A. Study Area

This study was conducted at Kali Ledug Watershed, located in Tangerang City, Indonesia, with geographical boundaries between 106° 33' 45" and 106° 36' 1" Eastern longitude and between -6° 9' 7" and -6° 13' 19" Southern latitude (Fig. 1). With an area of 14.43 km^2, the Kali Ledug Watershed falls in the Jatiuwung District (upstream) and Periuk District (downstream). Kali Ledug Watershed is a lowland area with an elevation range of 5 m downstream to 34.84 m upstream. This watershed is a flat area with an average slope of 3.23%. The main river in Kali Ledug Watershed is Kali Ledug, which flows from South to North.

As part of a city adjacent to Jakarta, the capital city of Indonesia, the Kali Ledug Watershed has experienced rapid regional growth. In the City Spatial Planning in 2012–2032, the Jatiuwung District is planned as an industrial area. Periuk District is projected to transform into an area conducive to trade and services, medium to high-density housing integrated industries with an environmental perspective [7]. Housing, industries, and other socio-economic facilities have rapidly developed and resulted in a land-use change over the last decades.

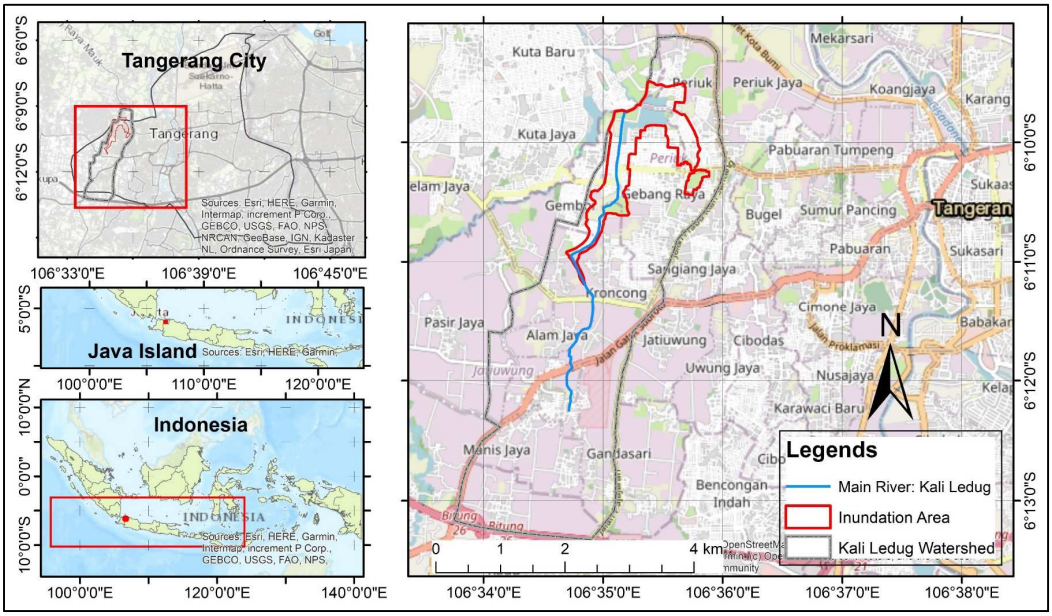

Fig. 1 The geographic location of the study area in Tangerang City, Indonesia

B. Conceptual Framework

Local authorities require information about the flood vulnerability of the watershed under their authority. This includes comprehensive information regarding the temporal change of watershed flood vulnerabilities and predictions of flood vulnerability growth due to future scenarios, one of which is based on rainfall scenarios with various return periods. For this reason, local authorities need information on the main contributing factors to the flood events in the watershed in order to evaluate the temporal change of flood vulnerability resulting from the built-up area increasing in the watershed and predict scenarios for flood vulnerability due to future rainfall over various return periods. This information would be helpful as input data for flood mitigation planning, a flood risk communicating tool to the public, and considerations in flood-based spatial planning.

Multi-criteria spatial analysis with criteria weighting could be used to determine the main factors causing flood vulnerability of a watershed [11], [12], [16], [17], [30]. Based on the valid model, the evaluation of flood vulnerability changes as a result of the growth of built-up areas due to human activities and public policies [31], [32], and the prediction of flood vulnerability changes due to rainfall with various return periods (10, 50, 100 years) could be conducted to obtain information that underlies the flood risk management policy in the watershed.

C. Method of Physical Flood Vulnerability Evaluation and Prediction

In this study, evaluating and predicting watershed flood vulnerability was carried out in four stages: stage one spatial data preparation, stage two criteria weighting using the AHP method, stage three multi-criteria analysis, and stage four, creating an evaluation model using land cover time-series data and prediction model using rainfall data with various return periods (Fig. 2). In stage one, the physical criteria used in the evaluation include elevation, slope, topographic wetness index (TWI), land cover, distance to the river, soil type, distance downstream, and rainfall. The physical criteria used in this study are the results of a literature study [11], [12], [16], adapted to the research area's physical conditions.

In the second stage, this study used AHP as a multi-criteria weighting method because studies have found that each criterion had a varied contribution to the flood vulnerability. The AHP method has been used by many studies to assign weighting criteria based on expert judgements. In the third stage, multi-criteria spatial analysis was conducted and validated using an accuracy assessment model based on flood inundation data in February 2020. The result of this stage was a valid model that described the condition of watershed flood vulnerability and the valid criteria weights during the flood event.

Many studies have used geospatial techniques and multi-criteria weighting methods to measure flood vulnerability, as described in stages one to three (Fig. 2). This study participated in the debate of scientific literature by adding stage four, the flood vulnerability evaluation and prediction modelling, conducted based on the valid model. The input data used in the flood vulnerability evaluation were time-series land-cover data from 2001 to 2020 with 5-year intervals. The model was run for each land cover from 2001 to 2020 to obtain time-series physical flood vulnerability. A correlation test was conducted between the built-up area and the area with high and very high flood vulnerability, and a regression equation was developed to represent such correlation.

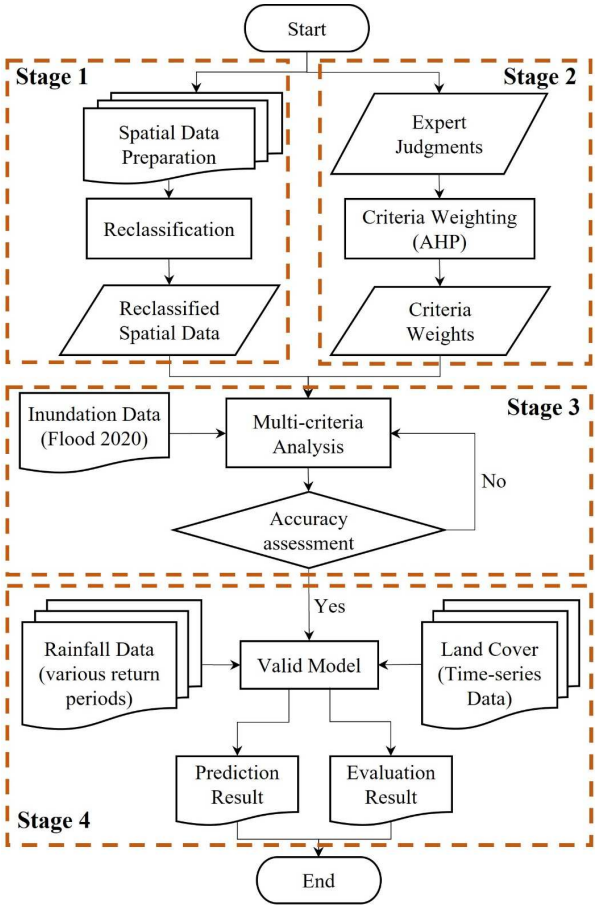

Fig. 2 Flowchart of the flood vulnerability evaluation and prediction

Rainfall data with various return periods ranging from 5 to 100-years were also used to determine the physical flood vulnerability based on the valid model. These prediction models produced flood vulnerability maps for various rainfall, proving useful in flood defense infrastructure planning. The local authorities could use the regression equation and the rainfall-based prediction to predict the increase in areas with high flood vulnerability levels due to the growth of the built-up area and the rainfall return period.

D. Spatial Data Preparation

The data used in this study was obtained from various sources. Data on watershed boundaries, elevation, slope, and TWI was obtained from the Indonesian National DEM (DEMNAS) image processing, which is DEM data with 0.27-arcsecond (8.3 m) resolution produced by the Indonesian Geospatial Information Agency (Badan Informasi Geospasial/BIG). Time-series land cover data were obtained from the Indonesian National Research and Innovation Agency (BRIN) based on Landsat 7 ETM images and Landsat 8 OLI images. As maximum daily rainfall data, soil type data was obtained from the local authorities, river spatial data from BIG, and rainfall data from the Indonesian Agency for Meteorological, Climatological, and Geophysics.

1) Elevation: Elevation is a significant factor in the physical flood vulnerability analysis. In most GIS-based flood vulnerability studies, this factor is used because of its significant influence on the formation of flood vulnerability [12], [13], [15], [33], [34]. In this study, the elevation data was obtained from DEMNAS data by clipping on the study area, ranging from 0–53.47 m (Fig. 3a).

2) Slope: Slope also plays a significant role in the physical flood vulnerability analysis, which is used in most GIS-based studies [12], [13], [15], [33]. Slope affects the speed of the water flow through drainage channels and watersheds. In the surface runoff formation, slope acts as the main factor so that, on flat surfaces (small slopes), water flows slower than on surfaces with large slopes [33], [34]. This study generated the slope from the DEMNAS data, ranging from 0.01 to 43.66% (Fig. 3b).

3) Topographic Wetness Index (TWI): Topographic Wetness Index represents the influence of the topographical conditions in each watershed raster cell during the formation of surface runoff [35], [36]. This criterion indicates whether a raster cell can topographically produce surface runoff or not. In general, TWI includes two things: the hydrographic position of the cell in the watershed and the presence or absence of a low slope. With SCA as a Specific Catchment Area and α as the slope angle, assuming uniform soil properties [35], TWI is calculated through Formula (1).

$$TWI = \ln \frac{SCA}{\tan \alpha} \quad (1)$$

Technically, TWI is generated based on DEMNAS data and ranged from 2.98 to 21.04 (Fig. 3c).

4) Distance to the river: Floods in the study area occur along with the river flow, so the distance to the river becomes an essential factor [11]. The area closest to the river is most vulnerable to flooding; therefore, the watershed area is divided into five classes based on the river criterion's distance. This study used a 100 m distance classification starting from the river channel. Euclidean Distance, a spatial analysis tool provided by ArcGIS, is used to obtain spatial data on the distance to the river.

5) Distance to downstream: Naturally, water flows to a place with a lower elevation so that if there is a flow barrier in the downstream area, there will be a build-up of flow discharge. This condition relates to the relationship between upstream and downstream areas in a watershed, which is complex and requires comprehensive research for better understanding [37]. The flood defense infrastructure program in the upstream area might increase flood discharge in the downstream area [38]. In this study, the area closest to the downstream was assumed to be most vulnerable to flooding. To obtain spatial data distance to the downstream, the spatial analysis method used was Euclidean Distance. The classification used a distance of every 1,000 m, starting from the estuary.

6) Soil type: The effect of soil type in a watershed on the formation of surface runoff is highly dependent on soil characteristics such as layer thickness, permeability, infiltration rate, and the level of soil moisture contained [34]. Technically, the infiltration rate of a location can be determined based on the soil type. In the study area, the soil type in all watershed areas was the associated of red latosol and reddish-brown latosol.

7) Land cover: Land cover is a significant factor in the analysis of physical flood vulnerability [12], [13], [15], [33], [34]. This study used land cover data from 2001 to 2020. The land cover data for 2001, 2006, and 2011 were produced based on Landsat 7 ETM imagery and for 2016 and 2020 based on Landsat 8 OLI imagery. The analytical method for determining land cover classification was supervised using the Random Forest (RF) algorithm. Land cover was classified into six classes: built-up area, barren land, dense vegetation, less dense vegetation, sparse vegetation, and water body (Fig. 3d). The analytical method identified land cover changes in the watershed; the built-up area increased significantly from 25.3% (2001) to 64.09% (2020), while other land cover areas decreased.

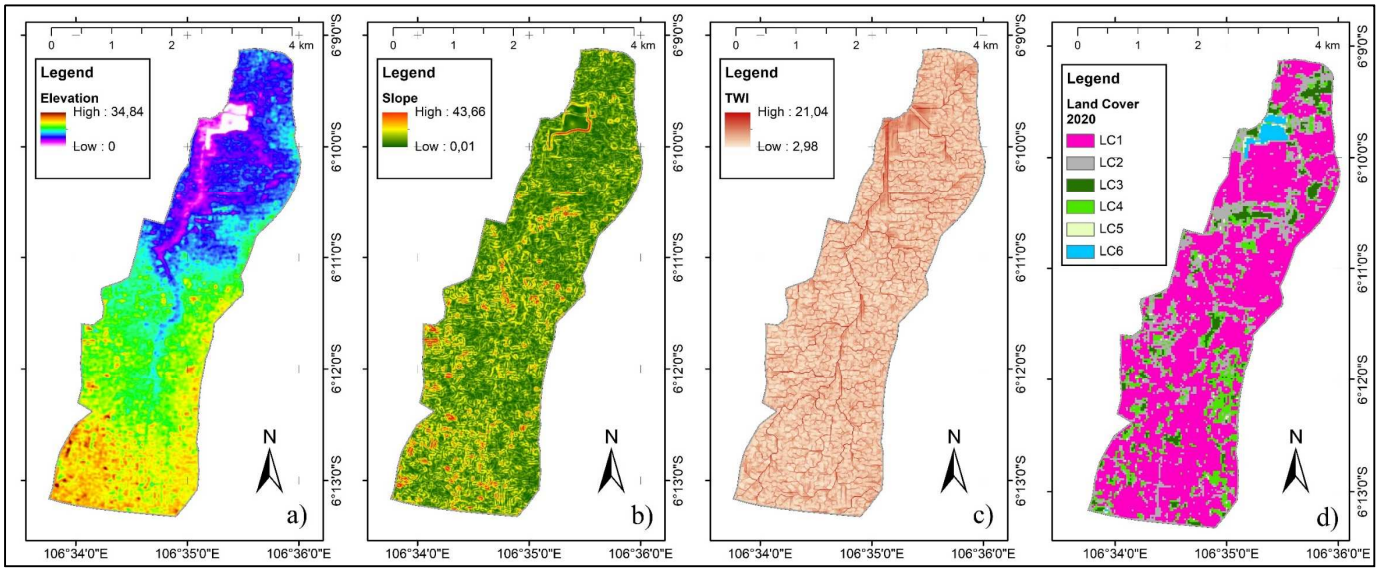

Fig. 3 Data preparation for the flood vulnerability evaluation and prediction model: a) elevation, b) slope, c) TWI, d) land cover (2020)

TABLE I
CRITERIA RECLASSIFICATION

Nr.	Criteria	Reclassification	Score	Level
1	Elevation (EL)	0-7 m	5	Very high
		7-14 m	4	High
		14-21 m	3	Moderate
		21-28 m	2	Low
		28-35 m	1	Very low
2	Slope (SL)	>45%	5	Very high
		25-45%	4	High
		15-25%	3	Moderate
		8-15%	2	Low
		0-8%	1	Very low
3	TWI (TW)	0-5	5	Very high
		5-10	4	High
		10-15	3	Moderate
		15-20	2	Low
		20-25	1	Very low
4	Land cover (LC)	Built-up area	5	Very high
		barren land	4	High
		sparse vegetation	3	Moderate
		less dense vegetation	2	Low
		dense vegetation	1	Very low
5	Distance to River (DR)	0-100 m	5	Very high
		100-200 m	4	High
		200-300 m	3	Moderate
		300-400 m	2	Low
		>400 m	1	Very low
6	Soil type (ST)	Regosol	5	Very high
		Alluvial, andosol	4	High
		Latosol, Litosol	3	Moderate
		Mediteran	2	Low
		Grumusol	1	Very low
7	Distance to downstream (DD)	0-1,000 m	5	Very high
		1,000-2,000 m	4	High
		2,000-3,000 m	3	Moderate
		3,000-4,000 m	2	Low
		> 4,000 m	1	Very low
8	Rainfall (RA)	200-230 mm	5	Very high
		170-200 mm	4	High
		140-170 mm	3	Moderate
		110-140 mm	2	Low
		77-110 mm	1	Very low

8) Rainfall: The maximum daily rainfall data were processed into regional rainfall for return periods of 2, 5, 10, 25, 50, and 100-years. As there are no rainfall stations within the Kali Ledug Watershed, it is necessary to perform spatial interpolation of data from several rainfall stations around the Kali Ledug watershed. The spatial interpolation method used was inverse distance weighting (IDW). The IDW method is considered one of the standard methods for obtaining interpolated data [39]–[41]. This method assumes that the value of the point located closer to the measurement location will be affected more by the value of the measurement point. This assumption assigns a smaller distance value a more significant weight value. In this study, the rainfall values ranged from 118.74 to 124.31 mm/d (5-year return period), while for the 100-year return period, the rainfall values ranged from 223.90 to 225.53 mm/d.

Furthermore, all spatial criteria must be reprojected, clipped and reclassified into the same scale to be mathematically operated. All criteria were reclassified for this flood vulnerability analysis into five classes ranging from 1 to 5 (TABLE I). After spatial criteria were reclassified, a weighted overlay analysis was performed, and the criteria weights were determined using the AHP method.

E. Criteria Weighting using AHP

The AHP method was used to describe complex decision-making problems using a hierarchical system [42]. In this study, criteria weighting analysis was performed to consider the effect of each variable on physical flood vulnerability. The AHP method was applied using three expert judgments, which assessed the pairwise comparison matrix between the criteria of the flood vulnerability. The score used in the pairwise comparison matrix ranged from 1 to 9 [42], where a value of 1 meant that an indicator had the same important value as its partner indicator, while a value of 9 meant that an indicator had an extremely important than its partner indicator. A value of 3 means moderate importance, a value of 5 means strongly importance, and a value of 7 means very strongly importance. For example, when comparing criteria A and B, the value 9, located on line B, meant that criterion B was more important than criterion A.

The expert's judgment could be different for each criterion during pairwise comparison; thus, for criteria weight analysis, with n is the number of experts and x_1, x_2, …, x_n are pairwise comparison values, the geometric mean (G_x) value was calculated using Formula (2) [42].

$$G_x = \sqrt[n]{x_1.x_2 \dots x_n} \quad (2)$$

The analysis in the AHP method was carried out in two stages: first, criteria weight analysis, and second, consistency assessment. Criteria weight analysis was performed by (i) calculating the normalisation value for each criterion and (ii) determining the normalised principal eigenvector or priority vector (also called relative weight). An iteration process was conducted to obtain the most accurate eigenvalues so that the difference in eigenvalues between the stages is close to zero. The normalised value in the matrix was the cell value divided by the column sum. This process produced a column sum value of 1 for each criterion. The relative weights were then calculated by averaging the rows of each matrix.

The consistency assessment was performed because of the possibility of judgment inconsistencies in the pairwise comparison assessment. In the AHP method, this inconsistency can be tested using the consistency ratio (CR), which is the ratio between the consistency index (CI) and the random index (RI).

$$CI = \frac{\lambda_{max} - n}{n-1} \quad (3)$$

$$CR = \frac{CI}{RI} \quad (4)$$

CI is a function of the maximum eigenvalue (λ_{max}) of the pairwise comparison matrix and the number of indicators used (n). RI represents the consistency index of the random pairwise comparison matrix. Saaty (2004) has provided a table of RI values that depend on the number of criteria used [42]. A CR value lower than 0.10 indicates consistency in the pairwise comparison assessment, so the result of the criteria weight analysis can be used [42].

III. Results and Discussion

A. Criteria Weighting

Based on the three expert judgments on criteria pairwise comparisons, a matrix containing the geometric mean of the assessment was compiled (TABLE II). Furthermore, this matrix was normalised by dividing each cell value by its column sums. At the end of this process, the initial eigenvalues were obtained, then used as a value for comparison with the eigenvalues of the following iteration process. In the first iteration process, the difference in the eigenvalues derived was significant (0.01–0.03), necessitating the second iteration process. In the second iteration stage, the difference in eigenvalues was close to zero; thus, the eigenvalues obtained in the second iteration process were used as criteria weights. The weighting analysis of the criteria using the AHP method resulted in elevation (16.42%), slope (8.15%), soil type (6.39%), TWI (8.73%), distance to the river (15.34%), rainfall (21.31%), land cover (11.02%), and distance to downstream (12.64%), respectively.

TABLE II
GEOMETRIC MEAN OF EXPERT JUDGMENTS

	EL	SL	ST	TW	DR	RA	LC	DD
EL	1.00	1.18	1.53	1.41	2.00	0.94	1.53	2.00
SL	0.85	1.00	1.73	1.22	0.71	0.20	0.33	0.58
ST	0.65	0.58	1.00	0.58	0.58	0.27	0.41	0.71
TW	0.71	0.82	1.73	1.00	0.41	0.58	1.00	0.58
DR	0.50	1.41	1.73	2.45	1.00	0.93	1.73	2.00
RA	1.07	4.90	3.74	1.73	1.08	1.00	3.46	0.82
LC	0.65	3.00	2.45	1.00	0.58	0.29	1.00	0.71
DD	0.50	1.73	1.41	1.73	0.50	1.22	1.41	1.00

The consistency ratio was calculated after the criteria weights were determined. In this study, the λ_{max} value was 8.5826. Based on Formula (3), with eight criteria and the λ_{max} value, the CI value was calculated as 0.083. The random index (RI) value taken from the table given by Saaty [42] was 1.41 for eight criteria [42]. Therefore, the consistency ratio (CR) was calculated based on Formula (4), producing a CR value of 5.9%. With a CR value of less than 10%, the weighting results using the AHP method could be considered suitable for further use [42].

B. Flood Vulnerability Model

After determining the criteria weights, spatial analysis using a multi-criteria evaluation technique was performed by assigning the criteria weights to each criterion. The spatial analysis resulted in a flood vulnerability map in raster format showing the Kali Ledug Watershed with various flood vulnerability levels. Two parameters were used to interpret the modelling results, namely A1 and A2. A1 is where the model produced a high vulnerability value but the area was not flooded, while A2 is where the model produced a high vulnerability value and the area was flooded. A combination of criteria weights was sought in this accuracy assessment to produce a minimum A1 and a maximum A2. In the flood vulnerability model using the criteria weights from the AHP method, the A2 value was 29.98%, and the A1 value was 0.56%. The optimal value for the valid model was obtained by changing the criteria weights, which combines the maximum A2 value and the minimum A1 value. The A2 value obtained for this model was 77.05%, and the A1 value was 26.72%. The criteria weights in this valid model are elevation (41%), slope (10%), soil type (1%), TWI (6%), distance to the river (20%), rainfall (7%), land cover (7%), and distance to downstream (8%). In this valid model, the area with a high level of flood vulnerability is 1,639,065 m2 (Table III).

TABLE III
FLOOD VULNERABILITY OF KALI LEDUG WATERSHED

Level	Vulnerability Level	Area in m^2	Area in %
1	Very low vulnerable	57,021	0.40
2	Low vulnerable	6,551,755	45.40
3	Moderately vulnerable	6,182,191	42.84
4	Highly vulnerable	1,639,065	11.36

C. Land Cover based Flood Vulnerability Evaluation

Once the valid flood vulnerability model validation is performed, it can be used to evaluate physical flood vulnerability. The flood vulnerability evaluation in this study used land cover data from 2001 to 2020, with an interval of five years. The areas with a high and very high flood vulnerability experienced a quasi-linear growth from 2001 to 2020. In 2001 the area with high and very high vulnerability was 1,233,334 ha; in 2006, it was 1,369,894 ha, and in 2020 it was 1,639,065 ha. Considering the social-economic growth in the study area, the land-use change in the built-up areas would continue. For this purpose, a regression analysis was performed to determine the relationship between the built-up area and the area with a high level of flood vulnerability.

The regression analysis produced a linear regression equation with a coefficient of determination r2 of 0.96. With x as the built-up area, the resulting equation was as follows:

$$y = 0.0616\,x + 1{,}034{,}446.7 \quad (5)$$

Since the r2 value is close to one, it can be concluded that the regression model is highly accurate in predicting results.

D. Flood Vulnerability Prediction Model

The Prediction model of the area's growth with a high level of flood vulnerability was performed using rainfall data over various return periods. The model produced a flood vulnerability map with various levels of vulnerability in the entire Kali Ledug Watershed (Fig. 4a-c). Areas with high flood vulnerability in the Kali Ledug Watershed showed an increase compared to the flood inundation data of Feb 2020. For the rainfall with a 10-year return period, it is predicted that there will be areas with a high vulnerability of 1,906,018 hectares, the rainfall with a 50-year return period of 2,282,718 hectares and the rainfall with a 100-year return period of 2,565,191 hectares.

E. Discussion

This study demonstrated that the criteria elevation and distance to the river, with criteria weights of 41% and 20%, were the dominant factors in the physical flood vulnerability analysis. Other criteria such as slope, distance to downstream, rainfall, land cover, TWI, and soil type played a minor role, with criterion weights of 10%, 8%, 7%, 7%, 6%, and 1%, respectively. This model result followed the field conditions where flooding occurs in the downstream area with the lowest elevation in the watershed.

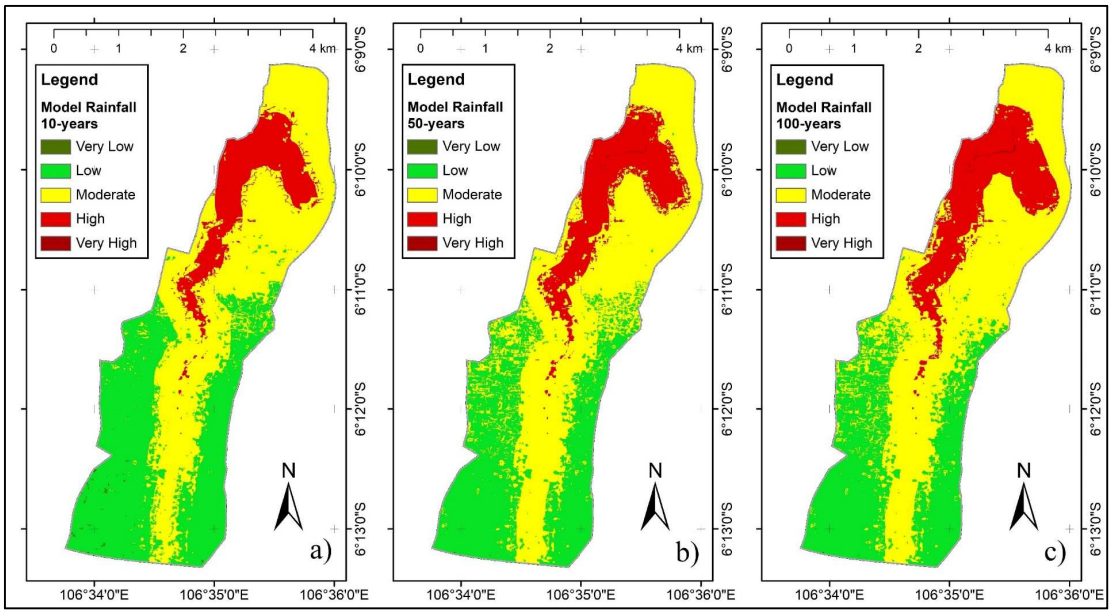

Fig. 4 Prediction of the area with high and very high flood vulnerability at various rainfall return periods: a) 10-year, b) 50-year, c) 100-year

Floods also occurred due to the overflow of Kali Ledug; thus, the distance to the river became significant. The criteria used in this study were relevant to those used in the literature, including land cover, elevation, slope, distance to the river, rainfall, drainage network, soil type, TWI, Stream Power Index (SPI), and Normalized Difference Vegetation Index (NDVI) [11]–[13], [15], [16], [18], [34]. While there is no definite agreement on which parameters should be applied for physical vulnerability analysis, there are some similarities in some of these studies. As in this study, the elevation factor and distance to the river were found to be the dominant factors in flood vulnerability by several studies [11], [13], [16]. In a study over a large study area (1,586 km^2) in Pakistan, Hussain et al. [13] found that the distance to the river played a dominant role (41%), followed by elevation (29%). In a study in Ethiopia covering an area of 1107 km^2, Desalegn & Mulu [16] found that the dominant variables were slope (37%) and elevation (25%). Desalegn & Mulu did not use the distance to the river as input data. In a study in India on a 6.46 km^2 watershed, Deepak et al. [11] found that the dominant variables influencing flood vulnerability are distance to the river (40%) and elevation (27%).

Several GIS-based flood vulnerability studies using AHP in criteria weighting did not critically assess the quality of criteria weights produced by the AHP method. Dandapat and Panda [19] used the weights generated by the AHP method to calculate the physical vulnerability index (PVI) and used the resulting PVI without validation. Ogato et al. [15] also used the AHP method for criteria weighting in calculating flood hazards. Using weights from the AHP method, the modelling results were also accepted without weight validation. In recent studies, several scholars also used the AHP method for variable weighting in calculating the flood vulnerability index but did not validate the criteria weights generated by the AHP method [11]–[13], [16]. We agree with Gigović et al. [33], who used three versions of the AHP method to weight the flood hazard criteria and validate the modelling results using inundation maps. The validation process recommended the AHP method with rough interval numbers as the weighting method with the highest accuracy. With almost the same method, Feloni et al. [12] used three variants of AHP and found that fuzzy-based AHP produced a model with a better accuracy level. However, neither Gigović et al. [33] nor Feloni et al. [12] did not modify the criteria weighting resulting from the AHP method.

This study validated the model with an inundation map by modifying the criteria weights produced using the AHP method. This weight modification was done to get the model results that fitted the validation data (inundation map). By changing some criteria weights, the model produced a higher level of accuracy. The AHP weighting method-based model produced a low accuracy level between the modelling results and the validation data in flooded areas (29.98%); in non-flooded areas, the model also produced small areas with a high vulnerability level (0.56%). Otherwise, the model with modified variable weights produced a high accuracy level between the modelling results and validation data in flooded areas (77.05%), and in non-flooded areas, this model produced moderate areas with a high level of vulnerability (26.72%).

Of the eight physical criteria used in the flood vulnerability analysis, only one criterion was directly affected by human activities: land cover. The built-up area played the highest role in increasing physical flood vulnerability among the land cover components, in line with the finding from Deepak et al. [11]. This information becomes the basis for answering questions about the effect of changes in built-up areas on flood hazard that has been occurring so far and how future physical development plans will affect flood susceptibility in the study area. Equation 5, $y = 0.0616\ x + 1{,}034{,}446.7$ can be used as a reference in analysing the impact of the physical development planning in the Kali Ledug Watershed. The increase of areas with high flood vulnerability (variable y) can be calculated based on the increase of the built-up area (variable x). The increase in areas with high vulnerability can be used as input for the local authority to plan relevant flood defence infrastructure to reduce the impact of flooding caused by growth in a built-up area.

Furthermore, the local authority can reduce the built-up area to reduce the area with high vulnerability. Practical solutions are appropriate land-use planning practices in flood-prone areas [16] and converting impermeable surfaces into vegetated land. In addition, predictions of areas with high vulnerability can also be used to communicate to the public about the flooding potential. Consequently, well-informed local authorities, communities, and other stakeholders can take mitigation actions and prepare themselves and the people for flooding [15]. Flood adaptive land-use planning supported by adequate infrastructure is expected to reduce the flood risk that hampers community activities [15], [27], [34] and ultimately reduce losses due to flooding [43].

As an implication at the operational level, the results of this study would support Grounds et al. [28], who found that people in flood-prone areas expect information about the potential for flooding. Flood vulnerability maps for several rainfall designs up to a return period of 100-years are critical as public communication tools regarding potential floods. In line with Grounds et al. [28], Intrieri et al. [29] found that information about potential floods is crucial for people living in areas with high flood vulnerability. The availability of flood vulnerability maps in those areas can increase public awareness in preparing for floods.

In this study, flood vulnerability prediction analysis and evaluation were demonstrated as a tool to generate flood vulnerability information needed by local authorities in managing watershed areas. We consider that the proposed method has worked well and could meet the expected goals. This study has provided insight to bridge research results to users at the operational level.

IV. Conclusion

This study evaluated and predicted the physical flood vulnerability of the Kali Ledug Watershed, Tangerang City, Indonesia, using GIS and AHP approaches by considering time-series land cover data and rainfall data over various return periods. It was found that the most significant factors in physical flood vulnerability are elevation (41%) and distance to the river (20%). The other criteria are slope (10%), distance to the estuary (8%), LULC (7%), rainfall (7%), TWI (6%), and soil type (1%), which played a minor role in the physical flood vulnerability. The evaluation model also recommended a formula (linear regression, $r^2 = 0.96$) to calculate the area with high flood vulnerability related to the built-up area to predict the impact of physical watershed development; therefore, the study result is essential for city planning. The vulnerability model was also used to predict the flood vulnerability level for several rainfall scenarios over various return periods up to 100-years, which are essential public communication tools for creating awareness regarding potential floods.

Another finding of this study was that using the AHP method for criteria weighting resulted in less-than-optimal model output than the validation data. Therefore, it was necessary to assess the model accuracy by modifying the criteria weights iteratively until the suitability of the model results and validation data reached the maximum. This study was conducted in a relatively small watershed (14.43 km^2). Therefore, studies in a broader study area and more heterogeneous flood events are necessary to increase generalizability. Moreover, since accuracy is a vital aspect of any model, we suggest further research using spatial data with higher resolution and more advanced validation techniques to improve the model accuracy.

Nomenclature

G_x	geometric mean	
m	number of experts	person
n	number of criteria	
x_n	pairwise comparison value expert n	
CI	consistency index	
RI	random index	

Greek letters

λ	eigenvalue	
α	slope angle	rad

Acknowledgment

This research and the article's publication were funded by the Grant PUTI Doktor 2020 from the Directorate of Research and Community Service, the University of Indonesia [grant number: NKB-746/UN2.RST/HKP.05.00/2020]. This research program was also supported by the Saintek-Scholarship program, The National Research and Innovation Agency (BRIN).

References

[1] Y. Lang and W. Song, "Quantifying and mapping the responses of selected ecosystem services to projected land use changes," *Ecol. Indic.*, vol. 102, no. July 2019, pp. 186–198, 2019, doi: 10.1016/j.ecolind.2019.02.019.

[2] C. Deng *et al.*, "How trade-offs between ecological construction and urbanization expansion affect ecosystem services," *Ecol. Indic.*, vol. 122, p. 107253, 2021, doi: 10.1016/j.ecolind.2020.107253.

[3] B. H. Santosa and R. H. Koestoer, "Public Green Space Planning and Management towards Livable City," in *2020 IEEE Asia-Pacific Conference on Geoscience, Electronics and Remote Sensing Technology (AGERS), 2020*, 2020, pp. 102–106. doi: 10.1109/AGERS51788.2020.945276.

[4] P. Riad, S. Graefe, H. Hussein, and A. Buerkert, "Landscape transformation processes in two large and two small cities in Egypt and Jordan over the last five decades using remote sensing data," *Landsc. Urban Plan.*, vol. 197, no. December 2019, p. 103766, 2020, doi: 10.1016/j.landurbplan.2020.103766.

[5] J. Hounkpè, B. Diekkrüger, A. A. Afouda, and L. O. C. Sintondji, "Land use change increases flood hazard: a multi-modelling approach to assess change in flood characteristics driven by socio-economic land use change scenarios," *Nat. Hazards*, vol. 98, no. 3, pp. 1021–1050, 2019, doi: 10.1007/s11069-018-3557-8.

[6] S. Vemula, K. Srinivasa Raju, and S. Sai Veena, "Modelling impact of future climate and land use land cover on flood vulnerability for policy support – Hyderabad, India," *Water Policy*, vol. 22, no. 5, pp. 733–747, 2020, doi: 10.2166/wp.2020.106.

[7] Tangerang City Government, "Tangerang City Regional Regulation Number 6 of 2019 concerning Amendments to Tangerang City Regional Regulation Number 6 of 2012 concerning the Tangerang City Regional Spatial Plan for 2012-2032," Tangerang City, 2019.

[8] Public Works and Public Housing Services, "Master Plan for Flood Control and Drainage System, Tangerang City," Tangerang City, 2017.

[9] J. Jian, D. Ryu, J. F. Costelloe, and C. H. Su, "Towards hydrological model calibration using river level measurements," *J. Hydrol. Reg. Stud.*, vol. 10, pp. 95–109, 2017, doi: 10.1016/j.ejrh.2016.12.085.

[10] N. Guo, X. Tang, Y. Ren, K. Ma, and J. Fang, "Place vulnerability assessment based on the HOP model in the middle and lower reaches of the Yangtze River," *GeoJournal*, vol. 86, no. 2, pp. 689–710, 2021, doi: 10.1007/s10708-019-10092-4.

[11] S. Deepak, G. Rajan, and P. G. Jairaj, "Geospatial approach for assessment of vulnerability to flood in local self governments," *Geoenvironmental Disasters*, vol. 7, no. 1, 2020, doi: 10.1186/s40677-020-00172-w.

[12] E. Feloni, I. Mousadis, and E. Baltas, "Flood vulnerability assessment using a GIS-based multi-criteria approach—The case of Attica region," *J. Flood Risk Manag.*, vol. 13, no. S1, pp. 1–15, 2020, doi: 10.1111/jfr3.12563.

[13] M. Hussain *et al.*, "Gis-based multi-criteria approach for flood vulnerability assessment and mapping in district Shangla: Khyber Pakhtunkhwa, Pakistan," *Sustain.*, vol. 13, no. 6, pp. 1–29, 2021, doi: 10.3390/su13063126.

[14] M. Nazeer and H. R. Bork, "A local scale flood vulnerability assessment in the flood-prone area of Khyber Pakhtunkhwa, Pakistan," *Nat. Hazards*, vol. 105, no. 1, pp. 755–781, 2021, doi: 10.1007/s11069-020-04336-7.

[15] G. S. Ogato, A. Bantider, K. Abebe, and D. Geneletti, "Geographic information system (GIS)-Based multicriteria analysis of flooding hazard and risk in Ambo Town and its watershed, West shoa zone, oromia regional State, Ethiopia," *J. Hydrol. Reg. Stud.*, vol. 27, no. March 2019, p. 100659, 2020, doi: 10.1016/j.ejrh.2019.100659.

[16] H. Desalegn and A. Mulu, "Flood vulnerability assessment using GIS at Fetam watershed, upper Abbay basin, Ethiopia," *Heliyon*, vol. 7, no. 1, p. e05865, 2021, doi: 10.1016/j.heliyon.2020.e05865.

[17] K. S. Vignesh, I. Anandakumar, R. Ranjan, and D. Borah, "Flood vulnerability assessment using an integrated approach of multi-criteria decision-making model and geospatial techniques," *Model. Earth Syst. Environ.*, vol. 7, no. 2, pp. 767–781, 2021, doi: 10.1007/s40808-020-00997-2.

[18] J. S. Cabrera and H. S. Lee, "Flood-prone area assessment using GIS-based multi-criteria analysis: A case study in Davao Oriental, Philippines," *Water (Switzerland)*, vol. 11, no. 11, 2019, doi: 10.3390/w11112203.

[19] K. Dandapat and G. K. Panda, "Flood vulnerability analysis and risk assessment using analytical hierarchy process," *Model. Earth Syst. Environ.*, vol. 3, no. 4, pp. 1627–1646, 2017, doi: 10.1007/s40808-017-0388-7.

[20] S. Chakraborty and S. Mukhopadhyay, "Assessing flood risk using analytical hierarchy process (AHP) and geographical information system (GIS): application in Coochbehar district of West Bengal, India," *Nat. Hazards*, vol. 99, no. 1, pp. 247–274, 2019, doi: 10.1007/s11069-019-03737-7.

[21] P. Ramkar and S. M. Yadav, "Flood risk index in data-scarce river basins using the AHP and GIS approach," *Nat. Hazards*, vol. 109, no. 1, pp. 1119–1140, 2021, doi: 10.1007/s11069-021-04871-x.

[22] M. Cerri, M. Steinhausen, H. Kreibich, and K. Schröter, "Are OpenStreetMap building data useful for flood vulnerability modelling?," *Nat. Hazards Earth Syst. Sci.*, vol. 21, no. 2, pp. 643–662, 2021, doi: 10.5194/nhess-21-643-2021.

[23] Y. Li, S. Gong, Z. Zhang, M. Liu, C. Sun, and Y. Zhao, "Vulnerability evaluation of rainstorm disaster based on ESA conceptual framework: A case study of Liaoning province, China," *Sustain. Cities Soc.*, vol. 64, no. February 2020, p. 102540, 2021, doi: 10.1016/j.scs.2020.102540.

[24] Ö. Ekmekcioğlu, K. Koc, and M. Özger, "District based flood risk assessment in Istanbul using fuzzy analytical hierarchy process," *Stoch. Environ. Res. Risk Assess.*, vol. 35, no. 3, pp. 617–637, 2021, doi: 10.1007/s00477-020-01924-8.

[25] H. Nasiri, M. J. M. Yusof, T. A. M. Ali, and M. K. B. Hussein, "District flood vulnerability index: urban decision-making tool," *Int. J. Environ. Sci. Technol.*, vol. 16, no. 5, pp. 2249–2258, 2019, doi: 10.1007/s13762-018-1797-5.

[26] S. Rashetnia and H. Jahanbani, "Flood vulnerability assessment using a fuzzy rule-based index in Melbourne, Australia," *Sustain. Water Resour. Manag.*, vol. 7, no. 2, pp. 1–13, 2021, doi: 10.1007/s40899-021-00489-w.

[27] A. Sahu, T. Bose, and D. R. Samal, "Urban Flood Risk Assessment and Development of Urban Flood Resilient Spatial Plan for Bhubaneswar," *Environ. Urban. ASIA*, vol. 12, no. 2, pp. 269–291, 2021, doi: 10.1177/09754253211042489.

[28] M. A. Grounds, J. E. Leclerc, and S. Joslyn, "Expressing flood likelihood: Return period versus probability," *Weather. Clim. Soc.*, vol. 10, no. 1, pp. 5–17, 2018, doi: 10.1175/WCAS-D-16-0107.1.

[29] E. Intrieri *et al.*, "Operational framework for flood risk communication," *Int. J. Disaster Risk Reduct.*, vol. 46, p. 101510, 2020, doi: 10.1016/j.ijdrr.2020.101510.

[30] M. Rahman *et al.*, "Flooding and its relationship with land cover change, population growth, and road density," *Geosci. Front.*, vol. 12, no. 6, p. 101224, 2021, doi: 10.1016/j.gsf.2021.101224.

[31] D. O. Onyango, C. O. Ikporukpo, J. O. Taiwo, and S. B. Opiyo, "Land use and land cover change as an indicator of watershed urban development in the Kenyan Lake Victoria basin," *Int. J. Sustain. Dev. Plan.*, vol. 16, no. 2, pp. 335–345, 2021, doi: 10.18280/IJSDP.160213.

[32] O. M. Ayenikafo and Y. F. Wang, "Land use/land cover changes analysis in sudano guinean region of benin," *Appl. Ecol. Environ. Res.*, vol. 19, no. 1, pp. 715–726, 2021, doi: 10.15666/aeer/1901_715726.

[33] L. Gigović, D. Pamučar, Z. Bajić, and S. Drobnjak, "Application of GIS-interval rough AHP methodology for flood hazard mapping in Urban areas," *Water (Switzerland)*, vol. 9, no. 6, pp. 1–26, 2017, doi: 10.3390/w9060360.

[34] X. Ren, N. Hong, L. Li, J. Kang, and J. Li, "Effect of infiltration rate changes in urban soils on stormwater runoff process," *Geoderma*, vol. 363, no. August 2019, 2020, doi: 10.1016/j.geoderma.2019.114158.

[35] P. Mattivi, F. Franci, A. Lambertini, and G. Bitelli, "TWI computation: a comparison of different open source GISs," *Open Geospatial Data, Softw. Stand.*, vol. 4, no. 1, 2019, doi: 10.1186/s40965-019-0066-y.

[36] R. Loritz *et al.*, "A topographic index explaining hydrological similarity by accounting for the joint controls of runoff formation," *Hydrol. Earth Syst. Sci.*, vol. 23, no. 9, pp. 3807–3821, 2019, doi: 10.5194/hess-23-3807-2019.

[37] S. Nepal, W.-A. Fluegel, and A. B. Shresta, "Upstream-downstream linkages of hydrological processes in the Himalayan region," *Ecol. Process.*, vol. 3, no. 19, pp. 1–16, 2014, doi: 10.1186/s13717-014-0019-4.

[38] D. T. Thu Ha, S. H. Kim, and D. H. Bae, "Impacts of upstream structures on downstream discharge in the transboundary imjin river basin, Korean Peninsula," *Appl. Sci.*, vol. 10, no. 9, 2020, doi: 10.3390/app10093333.

[39] Z. Li, "An enhanced dual IDW method for high-quality geospatial interpolation," *Sci. Rep.*, vol. 11, no. 1, pp. 1–18, 2021, doi: 10.1038/s41598-021-89172-w.

[40] Z. N. Liu, X. Y. Yu, L. F. Jia, Y. S. Wang, Y. C. Song, and H. D. Meng, "The influence of distance weight on the inverse distance weighted method for ore-grade estimation," *Sci. Rep.*, vol. 11, no. 1, pp. 1–8, 2021, doi: 10.1038/s41598-021-82227-y.

[41] W. yue Zou, S. qing Yin, and W. ting Wang, "Spatial interpolation of the extreme hourly precipitation at different return levels in the Haihe River basin," *J. Hydrol.*, vol. 598, p. 126273, 2021, doi: 10.1016/j.jhydrol.2021.126273.

[42] T. L. Saaty, "Decision making with the Analytic Hierarchy Process," *Int. J. Serv. Sci.*, vol. 1, no. 1, pp. 83–98, 2008, doi: 10.1504/IJSSCI.2008.017590.

[43] Z. Afifi, H. J. Chu, Y. L. Kuo, Y. C. Hsu, H. K. Wong, and M. Z. Ali, "Residential flood loss assessment and risk mapping from high-resolution simulation," *Water (Switzerland)*, vol. 11, no. 4, pp. 1–15, 2019, doi: 10.3390/w11040751.